

Reduced Chemical Mechanism for Methane Combustion

O.J.Haidn^o and N.A. Slavinskaya*

*Institute of Combustion Technology, Stuttgart,

^oInstitute of Space Propulsion, Lampoldshausen, German Aerospace Centre (DLR)

Abstract

A skeletal mechanism for methane combustion for the following operating conditions of pressure, temperature and mixture ratio - $0.1 \text{ MPa} < p < 6 \text{ MPa}$, $900 \text{ K} < T < 1800 \text{ K}$ and $1.0 < \Phi < 2.0$ - has been developed and validated applying an appropriate broad experimental data base. The model has 120 reactions of 27 species and predicts flame velocities and ignitions delays with less than 10% deviation from the results of the values obtained with the detailed model.

1. Introduction

Within the frame of the European Long Term Advanced Technologies (LAPCAT) program technologies are sought after which aim at the development of a high speed supersonic civil transportation system. Most likely, such a supersonic transport requires a high performance propulsion system and in order to predict with sufficient accuracy the combustion performance and the heat load to the combustion chamber walls of such advanced hydro-carbon fuelled engines, appropriate CFD codes with reliable chemical kinetic schemes are necessary. Unfortunately, all currently available reduced chemical kinetic models for methane combustion are too large to be implemented into 3D CFD tools applied for engine performance predictions [1-4].

There are a number of reasons why high pressure thrust chambers are operated in fuel-rich mode. Generally, the specific impulse will be higher since the molecular weight of the propellant is usually lower than that of the combustion product. However much more important are the extremely high heat loads which yield combustion chamber liner temperatures which exceed 800 K. Thrust chamber operation with lean mixture will therefore endanger the wall due to the surplus content of oxygen in the exhaust gases. As a consequence, fuel – rich operation is mandatory and thus soot formation in the combustion chamber has to be taken into account for both combustion performance and heat load to the walls since at temperatures above 3500 K radiation heat transfer may account for more than 40% of the total heat flux. Therefore, the model has to be able to predict precisely not only ignition delay and flame velocities at high temperatures and pressures but consequently also the formation of poly-aromatic hydrocarbons and finally soot.

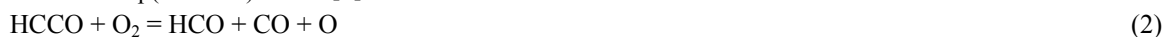
Prior to any modelling and reduction activities it is necessary to build an analytical and experimental data base which contains reliable data about chemical kinetic schemes and verification experiments in the entire field of operation regime of pressure, temperature and mixture ratio: $0.1 \text{ MPa} < p < 6 \text{ MPa}$, $900 \text{ K} < T < 1800 \text{ K}$ and $1.0 < \Phi < 2.0$. Three kinetic schemes [5 - 7] have been compared applying them to the data base mentioned above and one [6] was selected for further adaptation and reduction in the frame of the project LAPCAT. The presented paper reports results (i) of extensions and modifications of the model [6] performed to simulate flame speed and ignition delay for fuel-rich mixtures of methane and (ii) reduced mechanism obtained from produced kinetic scheme.

2. Chemical Kinetic Model

As the model under development has to describe the combustion of methane for a wide range of combustion chamber operating conditions, the kinetic scheme must be based on best set of validated thermo-chemical data with the minimum number of fitted data since these are generally very close to parameters for which the fitted kinetic data were obtained. After an intensive comparison of three kinetic mechanisms [5 - 7] which a preliminary study revealed as principally useful to describe the heat release in methane combustion under pressure $0.1 \text{ MPa} < p < 6 \text{ MPa}$, we selected as the base model for further development, the Leeds mechanism for methane oxidation [6]. This model is largely based on the set of recommended kinetic data [8, 9] with only a limited amount of optimized or fitted rate constants. Furthermore, the size of this model [6] is considerably smaller than the other two models [5, 7], a fact what is important for the further reduction process. First of all we adopted the recently updated [10] kinetic and thermodynamic data of the Leeds mechanism from newly reported data [9]. As these recent modifications [10] are performed for H_2 and CO chemistry, the basic Leeds model required some minor modifications and extensions to better describe methane oxidation and the main reaction paths leading to the formation of small molecules and radicals which important for PAH and soot growth, such as C_2H_2 and C_2H_3 . So, additionally to the reactions from [10] we included into the model the reaction



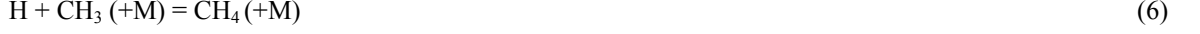
with $k_1 = 1.5 \cdot 10^7 T^{1.3} \exp(380.0/T)$ from [8], and the two channels for



with $k_{2,3} = 1.6 \cdot 10^{12} \exp(-430.0/T)$ from [9]. Second, the reaction $\text{CH}_2\text{CO} + \text{M} = \text{HCCO} + \text{H} + \text{M}$ was excluded from the model because the uncertainty of its reaction rate is even larger than its negative influence on the calculations of the flame velocities for CH_4 and C_2H_4 . Third, in order to improve the modelling of ignition delays for CH_4 we introduced for the reaction



the value $k_4 = 6 \cdot 10^{12} \exp(-12615.0/T)$ from [11], which is about two times smaller than the ones recommended in [57, 60]. For the pressure depended reactions



we applied the rate expressions based on the recommendations of [12] for high pressure methane oxidation. After modelling analysis we adopted for the reactions (5) and (6) the modified rate values $k_{\infty,5} = 6.2 \cdot 10^{16} T^{-1.0} \exp(-310.0/T)$ and $k_{\infty,6} = 2.5 \cdot 10^{16} T^{-0.5} \exp(-263.0/T)$. In order to improve the description of C_2H_3 formation we made the following changes to the reaction rates used in [6]. For the multi-channel oxidation of C_2H_3



the rate expression $k_7 = 1.12 \cdot 10^{14} T^{-0.833} \exp(-12786/T)$ from [13] and $k_8 = 4 \cdot 10^{12} \exp(-125/T)$ from [9]. For C_2H_3 formation through



we use reaction rate $k_9 = 2.35 \cdot 10^2 T^{3.63} \exp(-5670.0/T)$ from [9]. For the multi-channel reaction of acetylene with oxygen radical



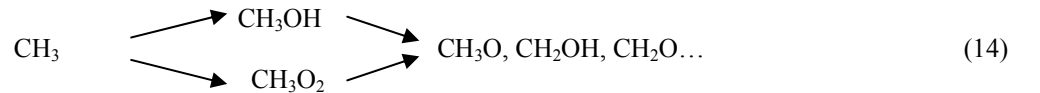
we use reaction rates $k_{10} = 1.6 \cdot 10^{14} \exp(-4990.0/T)$ of [14] and $k_{11} = 9.0 \cdot 10^{12} \exp(-2270.0/T)$ from [15]. In order to better describe the experimental data for ignition delay of methane at $T < 1100$ K and the flame speed data for lean mixtures we selected for reactions



two reaction rates, $k_{12} = 2.13 \cdot 10^{12} \exp(-12242.0/T)$ from experimental data [16] and $k_{12a} = 1.13 \cdot 10^{57} \exp(-8509.0/T)$ from reaction rate optimisation [19]. For the other important channel of CH_3O formation



the reaction rate $k_{\infty,13} = 1.1 \cdot 10^{11} T^{0.5} \exp(-1300.0/T)$ has been taken from [17]. As reported in [12, 17, 18] under the high pressure and low temperatures (1100 K) methyl radical reactions can have the following reaction routes:



In order to investigate the influence of these reaction paths we introduced into the mechanism two new species, CH_3OH and CH_3O_2 , and some reactions of CH_3O , CH_3CO , CH_2HCO and CH_3CHO from [12, 15, 17, 18], which are important for methane combustion. From experimental data for ignition delays of methanol, we evaluated the reaction rate for $\text{CH}_3\text{OH} + \text{O}_2 = \text{CH}_2\text{OH} + \text{HO}_2$ to be one order of magnitude smaller than that for $\text{CH}_3\text{OH} + \text{OH} = \text{CH}_2\text{OH} + \text{H}_2\text{O}$. The results of modelling and sensitivity analysis have shown that CH_3O_2 does not improve the low temperature ignition delay simulations and was thus deleted from the model.

3. Methods for Mechanism Reduction

3.1 Species elimination

The elimination of species decreases the dimensionality of the ODE system. A species may be considered redundant if its concentration change has no significant effect on the production rate of important species. The influence of a change of the concentration of species j on the rate of production of a p -membered group of important species i , can be taken into account by the sum of squares of the *overall normalized sensitivity coefficient* [20-21].

$$B_j = \sum_i^p \left(\frac{\partial \ln R_i}{\partial \ln c_j} \right)^2 \quad (15)$$

B_j yields the effect of a change of the concentration of species c_j on the rate of production of species i , R_i , from group of p important species, p is the number of important species given by the investigator. The higher the B_j value of a

species, the greater is its direct effect on important species. However, there are necessary species which influence the concentration of important species not through direct coupling but by influencing another necessary species which is so coupled. Thus, the group of necessary species has to be identified by an iterative procedure, which is realized in the package KINALC which we used for this analysis [21]. Within KINALC the numerical calculation of the concentration of derivatives is performed as follows:

$$c_{j+1} = c_j \times rtol + atol, \quad (16)$$

where $rtol = 1.0001$ and $atol = 1e^{-30}$.

In order to eliminate the unimportant species we calculated the sensitivity coefficients (14) for group of temperature and important species, which were selected after ordinary sensitivity analysis: T, CH₄, H₂, HO₂, CH₃, CH₂, OH, CH₃O as species important for ignition delay time and laminar flame speed determination. After each iteration step, KINALC calculates overall normalized sensitivity coefficient B_j (14) and adds the component with the greatest B_j to the group of important species and parameters. After the last iteration one can see the order in which the species have been added to the first main group. The last components we considered as redundant species. That analysis has been performed for 20 different calculations of ignition delay time and 8 laminar flame speed calculations, which cover the entire range of parameters of interest. The species which were unimportant simultaneously for all simulations have been eliminated from the mechanism.

3.2 Elimination of unimportant reactions

A classical and reliable method is the comparison of the contribution of reaction steps to the production rate of necessary species. A technique for the reduction of mechanisms, using reaction rates, is based on the sensitivity of production rates to changes in rate parameters. If these parameters are the rate constants and the reactions are considered irreversible, the normalized rate sensitivities have the form [20-21]:

$$[\tilde{F}(k,c)]_{ji} = \frac{\partial \ln R_j(k,c)}{\partial \ln k_i} = \frac{\alpha_{ji} w_i}{R_j} \quad (17)$$

α_{ji} is stoichiometric coefficients of species j in reaction i , R_j - the rate of production of species j , w_i - rate of reaction i , k_i - coefficient of reaction rate. Equation (17) shows that an element of the normalized rate sensitivity matrix is the ratio of the rate of formation or consumption of species j in reaction i , to the overall production rate of species j . In KINALC [21] the effect of changing the coefficient of reaction rate k_i on the rate of production of N - membered group of species i , R_i , using least squares objective function is considered. This approach leads to the application of the following overall sensitivity type measure [20]:

$$A_i = \sum_i^N \left(\frac{\partial \ln R_j}{\partial \ln k_i} \right)^2 \quad (18)$$

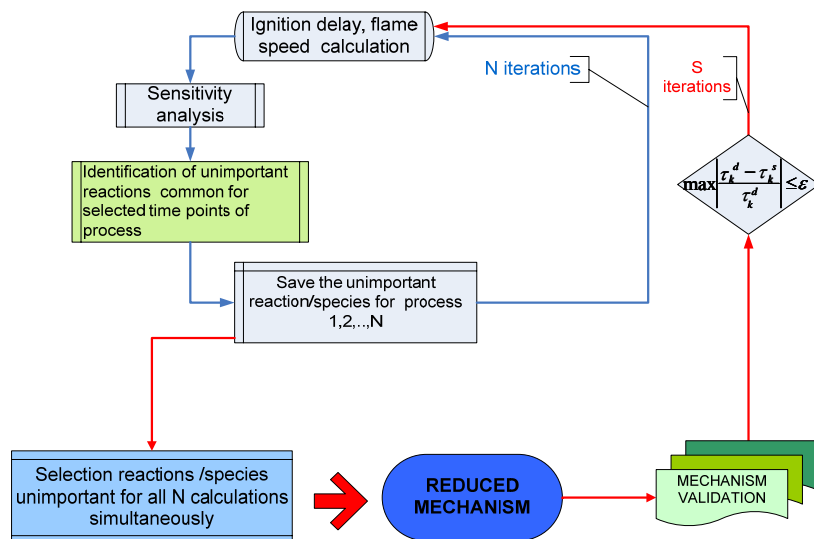


Fig.1. Scheme of iterative procedure for elimination of unimportant species and reactions.

A reaction i is considered as the important if its coefficients A_j , calculated as sum for all species, e.g. N is number of species in a model, are bigger than a chosen threshold $A_i \geq \Delta$. In order to computerize the selection procedure of unimportant reactions several additive modules to the KINALC package were developed. They define those unimportant reactions which are simultaneously unimportant for several simulations. For example, some calculations of ignition delays for different parameters and flame speed calculations. The modules eliminate the unimportant reactions from a mechanism, which are unimportant for all performed calculations. The unimportant reactions were selected with (17), (18), and $\Delta = 0.1$.

The elimination of unimportant species and reactions is the iterative procedure which has to be repeated several times until the simulations with reduced mechanism have the defined satisfactory agreement with experimental data, Fig1. After each elimination step, the reduced mechanism was validated with experimental data. On such way we obtained the skeletal mechanism which consists of 27 species and 127 reversible reactions and has disagreement with full mechanism not more than 10%.

4. Modelling Results

The key characteristic of any chemical kinetic scheme is its ability to predict ignition delay times and flame velocities. The latter is more important since flame velocities can be measured more precisely than ignition delay times. Typical experimental flame velocity data have generally errors which do not exceed 10%.

4.1 Ignition delay

We began the model validation with an examination of the chemistry of the new introduced species CH_3OH . That verification is also important for the chemistry of the CH_3O radical which is closely connected to them. The CH_3OH mechanism extension was examined, modelling experimental data of ignition delays for methanol [22] obtained in shock wave experiments for stoichiometric methanol mixture at pressure 1.35 MPa, and for $840 \text{ K} < T_0 < 1200 \text{ K}$, Fig.2. The model predicts quite satisfactory experimental data, but over-predicts the experimental data for low temperatures, $T_0 < 900 \text{ K}$. We have not found in presented model those reaction routes, which can promote only low temperature ignition without a worsening influence on middle and high temperature chemistry of CH_3OH oxidation.

For the mechanism validation on ignition delays we used experimental data [7, 19, 23, 24] obtained in shock tubes for

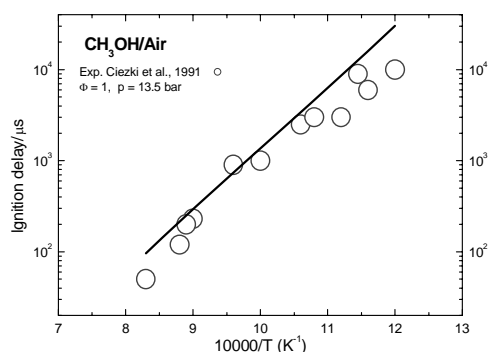


Fig.2. Comparison of modelled ignition delays for methanol/air with experimental data [22] for 1.35 MPa. Lines – simulations with presented mechanism LAPCAT.

fuel-rich methane mixtures under different pressures. The comparison with experimental data is presented on the Figs 3 – 6 for full and reduced models. These figures show as well the simulations with the other three originally considered mechanisms [5 - 7]. The maximum temperature gradient has been considered as reference point for ignition delay. The results of simulation are in good agreement with data [7] obtained for $\text{CH}_4/\text{O}_2/\text{Ar}$ mixtures with $\phi = 3$ under pressure 4.0 and 5.5 MPa, Fig.3 a, b.

For $\text{CH}_4/\text{O}_2/\text{Ar}$ mixture [23] with $\phi = 1.25$ under pressure 0.6 MPa, Fig.4 a, and for ignition of CH_4/air with $\phi = 1.0$ under pressure 1.7 MPa and 4.0 MPa, Fig.5 a,b, [19]. The full model over-predicts data [23] for pressure 1.0 MPa, Fig. 4 b, but the reduced mechanism has the good agreement with these experimental data. The model slightly underpredicts data [24] for $\text{CH}_4/\text{O}_2/\text{Ar}$ mixture with $\phi = 1.0$ under pressure 0.6 MPa and 1. MPa, Fig.6 a, b.

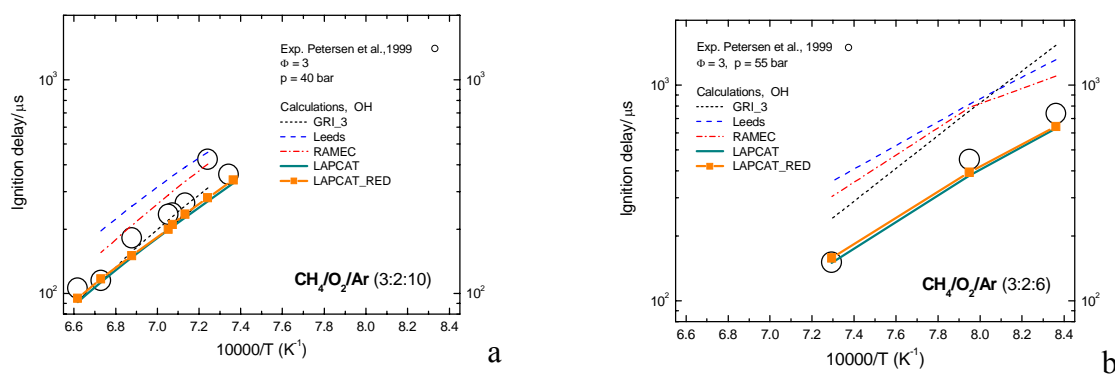


Fig.3. Comparison of modelled ignition delays of $\text{CH}_4/\text{O}_2/\text{Ar}$ mixtures, $\phi = 3$, with experimental data [7] for a) 4.0 MPa; b) 5.5 MPa. Lines – simulations with [5-7] and presented full and skeletal mechanism LAPCAT.

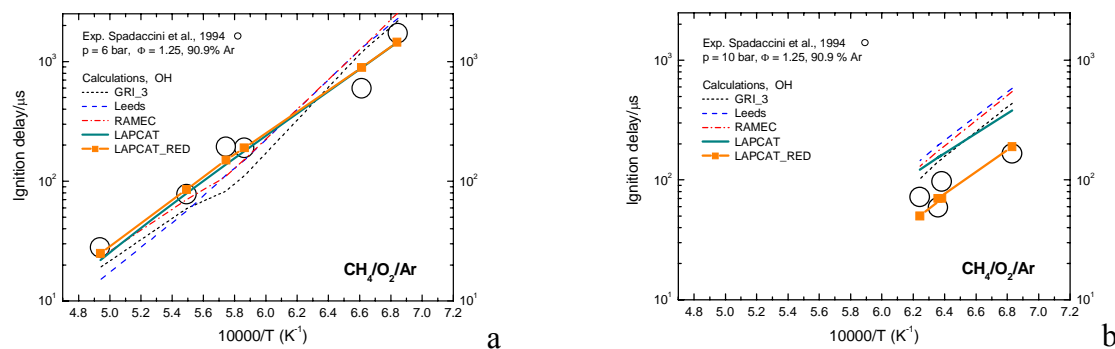


Fig.4. Comparison of modelled ignition delays of $\text{CH}_4/\text{O}_2/\text{Ar}$ mixtures, $\phi = 1.25$, with experimental data [23] for a) 0.6MPa; b) 1.0 MPa. Lines – simulations with [5-7] and full and skeletal mechanism LAPCAT.

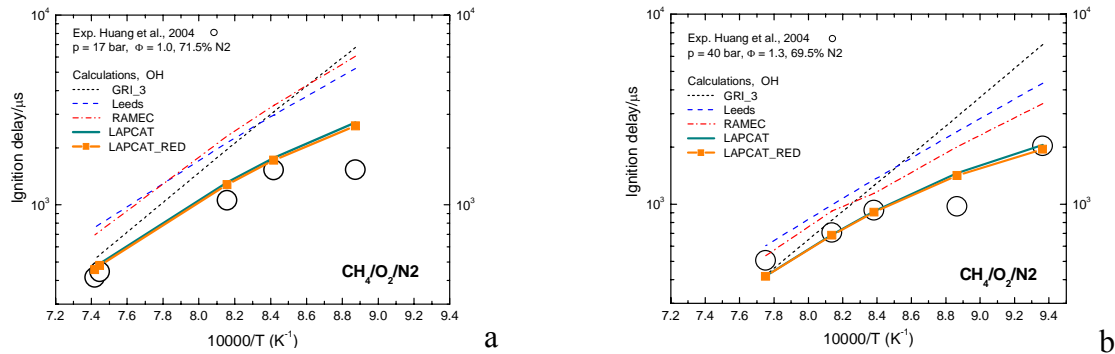


Fig.5. Comparison of modelled ignition delays of CH₄/Air mixtures, $\phi = 1.0$, with experimental data [19] for a) 1.7MPa; b) 4.0 MPa. Lines – simulations with [5-7] and full and skeletal mechanism LAPCAT.

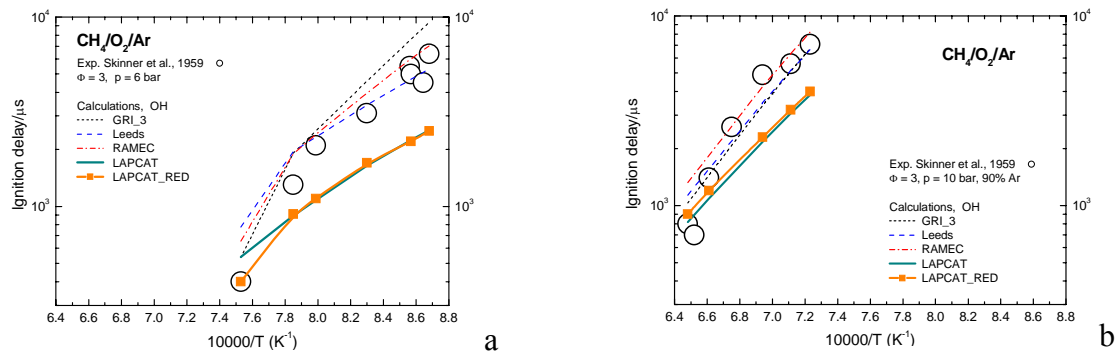


Fig.6. Comparison of modelled ignition delays of CH₄/O₂/Ar mixtures, $\phi = 3.0$, with experimental data [23] for a) 0.6MPa; b) 1.0 MPa. Lines – simulations with [5-7] and full and skeletal mechanism LAPCAT.

The sensitivity analysis [20] of OH radical concentration for two experimental points of [21] at 4.0 MPa, for lower temperature, 1068 K, and for higher one 1290 K, was performed in order to investigate the difference in reaction process, Fig.7 a, b. On the Fig.7 we show 20 reactions with the highest sensitivity coefficients.

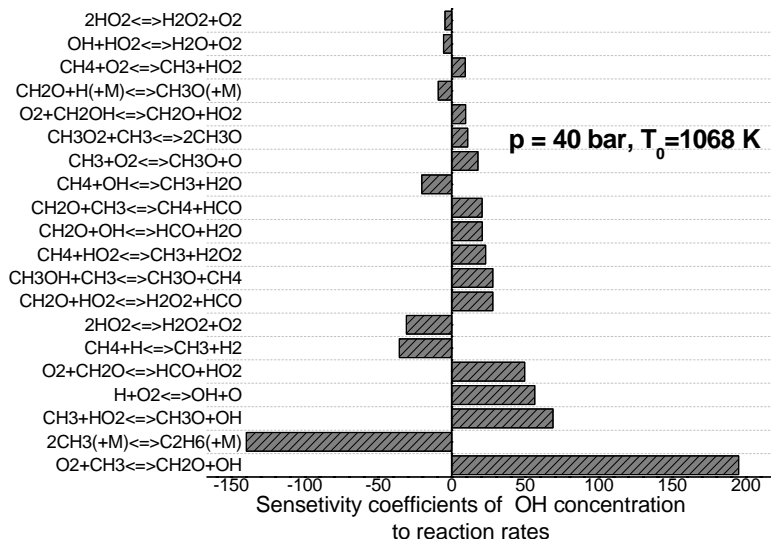
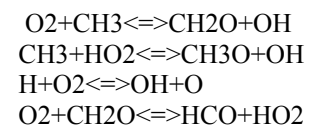


Fig.7 a: Sensitivity coefficients for ignition delay for $p = 4.0$ MPa and $\phi = 1.3$ (a) $T_0=1068$ K, (b) $T_0=1290$ K. Sensitivity coefficients calculated for $T = 1550$ K.

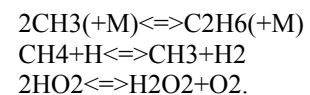
4.2 Flame speed

The comparison of high pressure flame speed simulations with experimental data [25-30] is presented on Figures 8-10. The LAPCAT models, full and reduced describes well the data for all pressures except for lean mixtures where a slight over-prediction occurs, see Fig.8-11, and for pressures higher than 6.0 MPa. The optimization of the rates which we made are for the reactions (5) and (6) are especially important for heat release in the methane system, is in good agreement with new kinetic data [10] for the principal combustion chemistry of H₂ and CO. Unfortunately, the kinetic data

In both cases the first most important reactions for OH radical production are nearly identical, but at lower initial temperature the sensitivity coefficients are in 10 times higher. The reactions promoting OH production are:



The reactions retarding the ignition delays are:



The reaction of methyl radical recombination has the highest negative sensitivity coefficient.

from the data base [8, 9] for methyl reactions (5) and (6) is somehow “incompatible” with new data for H₂ and CO. The implementation of these data leads to too high values for both ignition delays and flame velocities. The investigation of [3, 11, 12, 18], which we analysed for reaction rate optimization, give more realistic data for methyl recombination reactions.

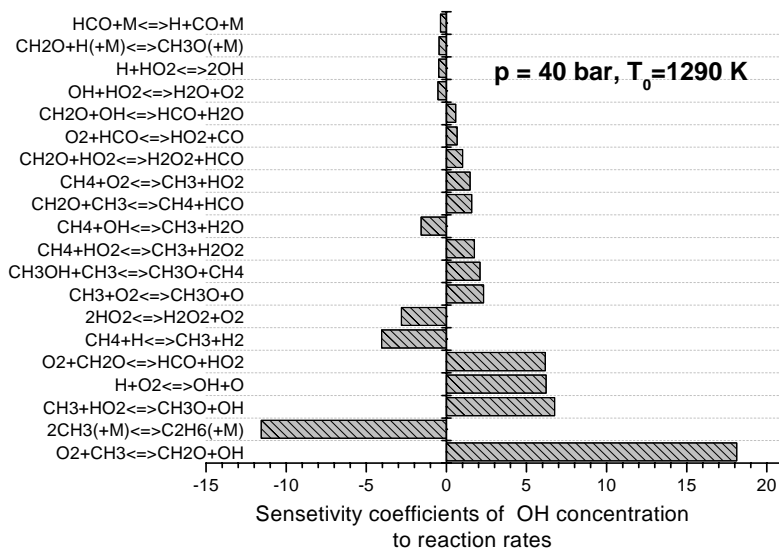


Fig.7b: Sensitivity coefficients for ignition delay for $p = 4.0$ MPa and $\phi = 1.3$ (a) $T_0=1068$ K, (b) $T_0=1290$ K. Sensitivity coefficients calculated for $T = 1550$ K.

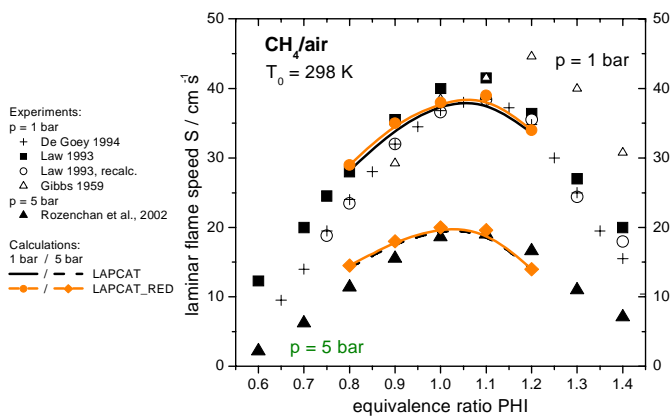


Fig.8. Laminar flame speed versus equivalence ratio of CH₄/air flames for 298 K and 0.1, 0.5 MPa. Symbols – experimental data [26-29], lines – simulations with detailed and skeletal mechanism LAPCAT

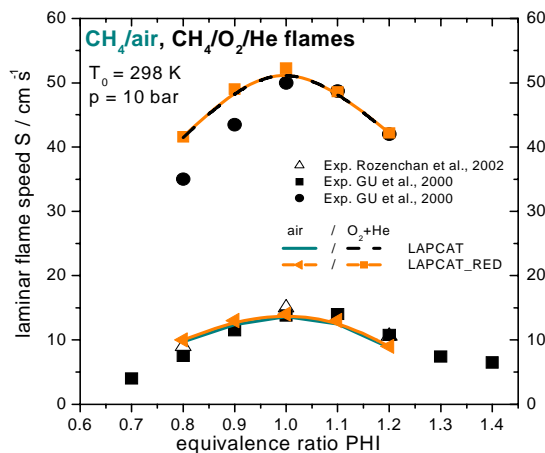


Fig.9. Laminar flame speed versus equivalence ratio of CH₄/air and CH₄/O₂/He flames for $T_0 = 298$ K and $p = 1.0$ MPa. Symbols-experimental data [25, 30], lines – simulations with detailed and skeletal mechanism LAPCAT

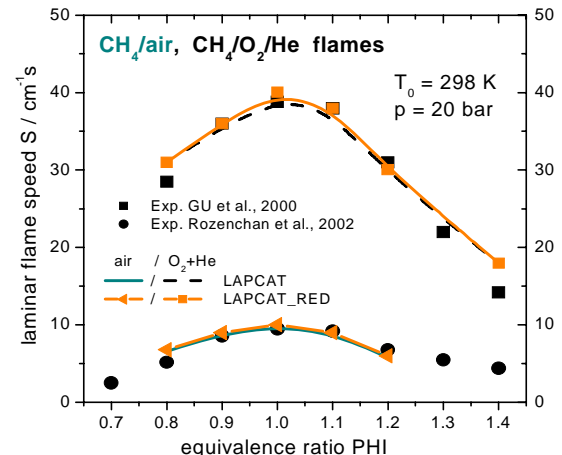
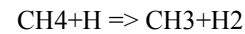


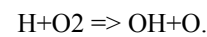
Fig.10. Laminar flame speed versus equivalence ratio of CH₄/air and CH₄/O₂/He flames for $T_0 = 298$ K and $p = 2.0$ MPa. Symbols-experimental data [25, 30], lines – simulations with detailed and skeletal mechanism LAPCAT.

The 20 highest sensitivity coefficients of flame speed to reaction rates calculated for pressures below 4.0MPa are shown on Fig.12. While the ignition delay is more sensitive to methyl recombination (5) and almost insensitive to reactions of methyl with hydrogen atom (6), Fig.7, the flame speed is mostly retarded through reaction of methyl with hydrogen atom (6) and is almost insensitive to methyl recombination (5), Fig. 12.

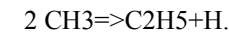
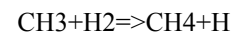
The second reaction with negative sensitivity coefficient is



Reactions of C_xH_yO_z species do not influence the flame speed and the most important reaction for flame speed under different parameter of process is:



As a consequence, the next most important reactions are reactions of H radical production:



So both directions of reaction $\text{CH}_4 + \text{H} = \text{CH}_3 + \text{H}_2$ are important for laminar flame velocity.

The reactions presented on Figures 7 and 12 are typically important reactions for all simulated processes. The relative importance of these reactions varies for different boundary conditions. As the model validation shows, the kinetic mechanism based mostly on the “first principals” of thermo-kinetic data reflects the main properties of heat release of high pressure combustion of fuel-rich methane flames. The model needs the further extensions to better predict ignition delays for initial temperature lower than 1100 K and laminar flame speed for lean mixtures and mixtures under pressure higher then 5 MPa.

6. Conclusions

After detailed investigation into the physical and kinetic details of the three mechanisms, Leeds, GRI 3.0 and RAMEC, the Leeds mechanism has been selected as the basic reaction model for development of the improved kinetic mechanism for methane combustion with high stoichiometric ratios and under high pressure. The Leeds mechanism is the smallest one and has the best physical and kinetic data base. The mechanism is developed to model heat release in combustors.

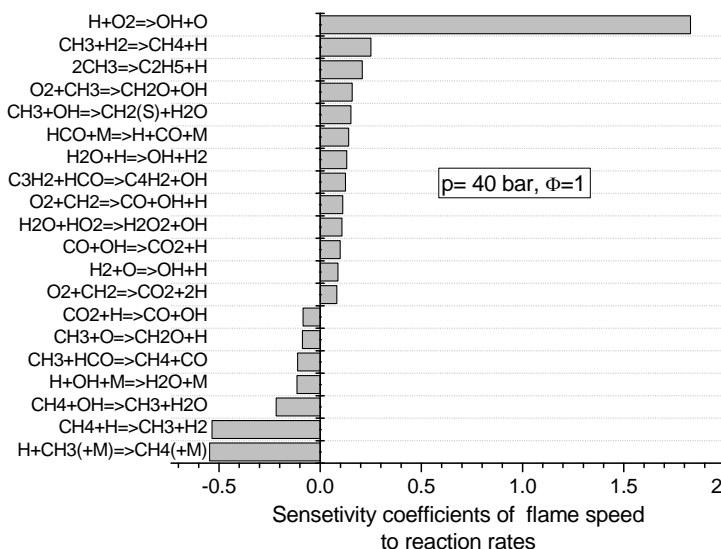


Fig. 12. Sensitivity coefficients for flame speed to reaction rates calculated for $p = 4.0$ MPa and $\phi = 1.0$

The models were intensively verified on large experimental data sets. The model describes satisfactory experimental data for ignition delay time $T_0 = 900 - 1400$ K, $p_0 = 1.0 - 6.0$ MPa, $\phi = 1.0 - 3.0$ and flame speed for $T_0 = 298$ K, $p = 0.10 - 6.0$ MPa, $\phi = 0.8 - 1.3$.

The presented mechanism has to be further improved in order to improve predictive capabilities for ignition delays for temperature below $T_0 < 1100$ K and laminar flame speed for lean mixtures and mixtures under pressure higher then 50 bar. Additionally, the full mechanism can be further extended to model the formation of soot for high pressure combustion and the skeletal model can be used to construct a global model for heat release modelling.

Acknowledgements

The work presented was partly financed and performed within the ‘Long-Term Advanced Propulsion Concepts and Technologies’ project investigating high-speed airbreathing propulsion. LAPCAT, coordinated by ESA-ESTEC, is supported by the EU within the 6th Framework Programme Priority 1.4, Aeronautic and Space, Contract no.: AST4-CT-2005-012282. Further info on LAPCAT can be found on <http://www.esa.int/techresources/lapcat>.

References

1. Revel J., Boettner J.C., Cathonnet M., Bachman J. S., “Derivation of a global kinetic mechanism for methane ignition and combustion,” *J. Chem. Phys.*, 1994, V. 91, pp. 365-382.
2. Kazakov A., Frenklach M., GRI 1.2_red, 1995, <http://www.me.berkeley.edu/drm/>.

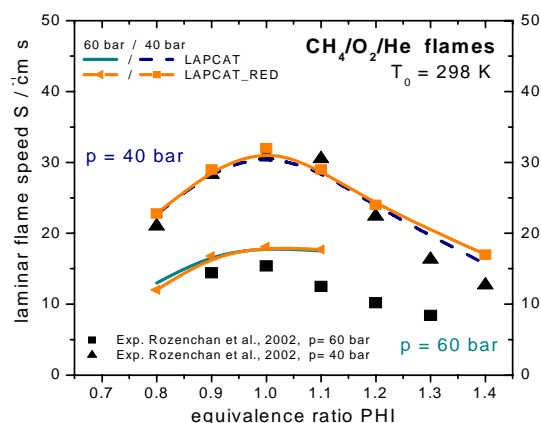


Fig. 11. Laminar flame speed versus equivalence ratio of $\text{CH}_4/\text{O}_2/\text{He}$ flames for $T_0 = 298$ K and $p = 4.0$ and 6.0 MPa. Symbols-experimental data [25], lines – simulations with detailed and skeletal mechanism LAPCAT.

for further reduction for implementation in CFD code

The following extensions and modifications of the basic mechanism have been performed:

- incorporation of updated reaction rates for H_2/CO submechanism;
- model improvement with new reaction rates for some important reactions;
- model improvement with additional reactions which are important for methane combustion for the conditions mentioned above ;
- model improvement with implementation of new species, CH_3OH and reactions for CH_3O , CH_3CO , CH_2HCO and CH_3CHO
- model reduction to obtain the skeletal mechanism which has facilities of input full model.

A chemical kinetic model for the CH_4/air combustion with 301 reactions and 39 chemical species and skeletal mechanism with 127 reactions and 27 species were developed to model heat release in the combustion chamber. The

3. Petersen E.L., Hanson R.K., "Reduced kinetics mechanisms for Ram accelerator combustion", *J. of Propulsion and Power*, 1999, V.15, pp.591-600.
4. Li S.C., Williams F.A., "Reaction mechanisms for methane ignition", ASME 2000, 2000-GT-145.
5. Smith G.P., Golden D.M., Frenklach M., Moriarty N.W., et al., GRIMECH 3.0 http://www.me.berkeley.edu/gri_mech/.
6. Hughes K.J., Turanyi T., Clague A.R., Pilling M.J., "Development and testing of a comprehensive chemical mechanism for the oxidation of methane", *Int. J. Chem. Kinet.*, 2001, V. 33, pp. 513-538.
7. Petersen E.L., Davidson D.F., Hanson R.K., "Ignition delay times of Ram accelerator CH₄/O₂/ diluent mixtures", *JPP*, 1999, V. 15, No1, pp.82-91.
8. Baulch D.L., Cobos C.J., Cox R.A., Frank P., Hayman G., Just Th., Kerr J.A., Murrells T., Pilling M.J., Troe J., Walker R.W., Warnatz J., "Evaluated kinetic data for combustion modelling supplement I", *J. Phys. Chem. Ref. Data* 23 (1994), pp. 847-1031
9. Baulch D.L., Bowman C. T., Cobos C.J., Cox R.A., Just Th., Kerr J.A., Pilling M.J., Stocker D., Troe J., Tsang W., Walker R.W., Warnatz J., "Evaluated kinetic data for combustion modelling: supplement II", *J. Phys. Chem. Ref. Data*, V. 34, 757 No. 3, 2005.
10. Zsély I.Gy., Zádor J., Turányi T., "Uncertainty analysis of updated hydrogen and carbon monoxide oxidation mechanism", *Proc. Combust. Inst.*, 30, 2005, pp.1273–1281.
11. Hunter T. B., Wang H., Litzinger T. A. and Frenklach M., "The oxidation of methane at elevated pressures: Experiments and modeling", *Comb. and Flame*, 1994, V.97, pp. 201-224.
12. Hall J. M., Petersen E.L., "Development of a chemical kinetics mechanism for CH₄/H₂/air ignition at elevated pressures", 2005, AIAA 2005-3768.
13. Lindstedt R.P., Skevis G., "Molecular growth and oxygenated species formation in laminar ethylene flames", *Proc. Combust. Inst.*, 28, 2000, pp.1801-1807.
14. Frank P., Bhaskaran K.A., Just T., "Acetylene oxidation: The reaction C₂H₂ + O at high temperatures", *Proc. Combust. Inst.*, 21, 1986.
15. Tsang W., Hampson R.F., "Chemical kinetic data base for combustion chemistry. Part I. Methane and related compounds", *J. Phys. Chem. Ref. Data*, 1986, V.15.
16. Braun-Unkloff M., Naumann C., Frank P., "A shock tube study of the reaction CH₃+O₂", *Proc. 20th Shock Waves Conference*, Marceille, 1993, pp.203-208.
17. Lindstedt R.P. and Meyer M.P., "A Dimensionally Reduced Reaction Mechanism for Methanol Oxidation", 2002.
18. Curran H.J., Gallagher S.M., Simmie J.M., "A comprehensive modelling study of methane oxidation", 2003, *Proc. Europ. Comb. Meeting*.
19. Huang J., Hill P. G., Bushe W. K., and Munshi S. R, *Comb. and Flame*, 2004, V.136, pp. 25-42.
20. Tomlin A.S., Turányi T., Pilling M.J. "Mathematical tools for the construction, investigation and reduction of combustion mechanism. *Comprehensive chemical kinetics*," Elsevier, 1997, V. 35, pp.293-437.
21. KINALC version 1.71; see <http://www.chem.leeds.ac.uk/Combustion/Combustion.html> or (Turanyi et al.) <http://garfield.chem.elte.hu/Combustion/Combustion.html>
22. Adomeit G., Fieweger K., Ciezki H., SFB 224, "Motorische Verbrennung", RWTH Aachen, 1991.
23. Spadaccini L.J., Colket M.B., "Ignition delay characteristics of methane fuels", *Prog.Energy Combust.Sci.*, 1994, V.20, pp. 431 – 460.
24. Skinner G.B., Ruehrwein R.A., "Shock tube studies on the pyrolysis and oxidation of methane", *J. of Phys. Chem.* 1959, V.63, pp. 1736-1742.
25. Rozenchan G., Zhu D. L., Law C.K., and Tse S.D., "Outward propagation, burning velocities, and chemical effects of methane flames up to 60 atm", *Proc. Combust. Inst.* 29, 2002, pp. 1461-1469.
26. Van Maaren A., Thung D.S., De Goey L.P., "Measurement of Flame Temperature and Adiabatic Burning Velocity of Methane / Air Mixtures", *Comb. Sci. and Techn.*, 1994, V.96, pp. 327-344.
27. Gibbs G.J., Calcote H.F., "Effect of Molecular Structure on Burning Velocity", *J. Chem. Eng. Data*, 1959, V4 (3), pp. 226 – 237.
28. Zhu D.L., Egolfopoulos, F.N., Law, C. K., "Experimental and Numerical Determination of Laminar Flame Speeds of Methane/(Ar, N₂, CO₂)-Air Mixtures as Function of Stoichiometry, Pressure, and Flame Temperature", *Proc. Combust. Inst.* 22, 1988, pp. 1537 – 1545.
29. Hassan M.I., Aung K.T., Faeth G.M. "Measured and Predicted Properties of Laminar Premixed Methane/Air Flames at Various Pressures", *Comb. and Flame*, 1998, V.115, pp.539–550.
30. Gu X. J., Haq M. Z., Lawes M., and Woolley R., "Laminar burning velocity and Markstein lengths of methane-air mixtures", *Comb. and Flame*, 2000, V.121, pp. 41-58.



This page has been purposely left blank